

## Summary of professional accomplishments

1. First name and surname: **Cezary Migaszewski**

2. University diplomas, scientific/artistic degrees – including the name, place and year as well as the title of the doctoral dissertation:

- Master's degree in astronomy, given by the Faculty of Physics, Astronomy and Informatics of the Nicolaus Copernicus University, Toruń, 2007.
- Doctor's degree of physical sciences in the field of astronomy, given by the Scientific Council of the Faculty of Physics, Astronomy and Informatics of the Nicolaus Copernicus University, Toruń, 2010. The dissertation title "Secular dynamics of planetary and stellar systems".

3. An information on employment in scientific/artistic institutions:

- 01.10.2009 – 30.09.2012: research-and-teaching assistant, Centre for Astronomy, Nicolaus Copernicus University.
- 01.10.2012 – 30.09.2016: assistant professor, Centre for Astronomy, Nicolaus Copernicus University.
- 01.02.2014 – 31.01.2017: post-doctoral researcher, Institute of Physics, University of Szczecin.
- since 02.02.2017: assistant professor, Centre for Astronomy, Nicolaus Copernicus University.

4. An indication of the achievement in accordance with art. 16 par 2 of the Act from March 14th 2003 on the scientific degrees, the scientific title and the degrees and the title in the filed of art (Dz. U. [Journal of Law] from 2016 item 882 as amended in Dz. U. from 2016 item 1311):

a) The title of the scientific/artistic achievement:

**Migration, periodic orbits and formation of mean motion resonances in systems with two and more planets**

b) The list of scientific articles constituting the achievement (author/authors, title/titles of publications, year of publication, publisher's name, publishing reviewers):

- H1 K. Goździewski, **C. Migaszewski**, "Multiple mean motion resonances in the HR 8799 planetary system", 2014, Monthly Notices of the Royal Astronomical Society, 440:3140–3171.
- H2 **C. Migaszewski**, "On the migration of two planets in a disc and the formation of mean motion resonances", 2015, Monthly Notices of the Royal Astronomical Society, 453:1632–1643.
- H3 **C. Migaszewski**, "On the migration of three planets in a protoplanetary disc and the formation of chains of mean motion resonances", 2016, Monthly Notices of the Royal Astronomical Society, 458:2051–2060.
- H4 **C. Migaszewski**, "On the migration-induced formation of the 9:7 mean motion resonance", 2017, Monthly Notices of the Royal Astronomical Society, 469:1131–1146.
- H5 **C. Migaszewski**, K. Goździewski, "A periodic configuration of the Kepler-25 planetary system", 2018, Monthly Notices of the Royal Astronomical Society, 480:1767–1777.

c) Discussion of the scientific/artistic goal of the publications listed above as well as the results achieved and their potential application.

## Introduction

Formation of planetary systems is an important issue of modern astronomy. Theories which describe the process focus both on the origin of planets in protoplanetary discs as well as on shaping the orbits and, for systems with more than one planet, forming the orbital configurations. Mean motion resonances (periodic orbits in particular) as well as planetary migration play a crucial role in the process. These concepts, listed in the title of the scientific achievement, will be explained further in the Introduction.

The planet-disc interaction results in an exchange of the mechanical energy and the angular momentum between the planet and the disc, which causes variation of the orbit size (the semi-major axis  $a$ ) and shape (the eccentricity  $e$ ). Although the character of the  $a$  and  $e$  changes depend on the disc parameters as well as on the mass and the orbit of the planet, in typical situations both  $a$  and  $e$  decrease, i.e., the migration is inward (the planet migrates towards the star) and the orbit is being circularised. The planet-disc interaction is the subject of many studies (e.g., Goldreich and Tremaine, 1979, 1980; Tanaka et al., 2002; Tanaka and Ward, 2004; Paardekooper et al., 2010, 2011). One of their goals is to determine the time-scales of migration  $\tau_a$  and circularisation  $\tau_e$ , when the disc parameters are given (instead of the pair  $\tau_a$  and  $\tau_e$  one often uses the quantities  $\tau_a$ , denoted simply with  $\tau$ , and  $\kappa \equiv \tau_a/\tau_e$ ). Another important aspect of the studies is the evolution of the disc itself (e.g., Shakura and Sunyaev, 1973; Pringle, 1981; D'Alessio et al., 1998). In general, one needs to consider the migration of planets in an evolving disc, i.e., the migration and circularisation rates are functions of the position of the planets in the disc as well as time (the disc evolutionary stage).

If in a given disc there are more planets of semi-major axes  $a_i$  and corresponding orbital periods  $P_i$  (where  $i$  enumerates the planets such as  $a_i < a_{i+1}$ ), the migration of a given pair may be convergent or divergent. The convergent migration of planets  $i$  and  $j$  ( $i < j$ ) means that planet  $j$  migrates faster than planet  $i$ , therefore the ratio of the semi-major axes  $a_j/a_i$  (as well as the period ratio  $P_j/P_i$ ) decreases in time. For the divergent migration, planet  $i$  migrates faster and  $a_j/a_i$  (and  $P_j/P_i$ ) increases in time.

It is known that the convergent migration results in formation of mean motion resonances, MMR, (e.g., Snellgrove et al., 2001; Lee and Peale, 2002), i.e., commensurabilities of the fundamental frequencies related to the orbital motion:  $n_i/n_j = P_j/P_i \approx (p+q)/p$ , where  $j > i$ , while  $p$  and  $q$  are small natural numbers, and  $q$  determines the order of the resonance;  $n_k \equiv 2\pi/P_k$  denotes the mean motion of planet  $k = i, j$ . The resonance relies on the synchronisation of the planets' motions as well as the variations of the orbital elements caused by the planet-planet interactions, i.e., semi-major axes, eccentricities, longitudes of pericentres, especially their difference  $\Delta\omega \equiv \omega_i - \omega_j$ , as well as the so called resonant angles  $\phi \equiv p\lambda_i - (p+q)\lambda_j + (q-r)\omega_i + r\omega_j$ , where  $\lambda_k$  is the mean longitude of planet  $k$  and  $r$  is a natural number from 0 to  $q$ . The behaviour of the  $\Delta\omega$  and  $\phi$  angles indicates whether or not the motions are synchronised. For the resonant configurations the angles should oscillate around fixed values. The synchronisation results in regular and stable evolution of the system. The latter is important because of the existence of chaos in the region of the resonance separatrix. The chaotic part of the phase space is larger, when the planets' masses are larger. In particular, lack of synchronisation of the system whose  $P_2/P_1 \approx (p+q)/p$  may result in chaotic evolution of the configuration, which may lead to destabilisation of the system.

Figure 1 presents an example evolution of the period ratio in a case of the convergent and divergent migration in a system of two planets  $i = 1, j = 2$ . The simulations were performed with a help of the so called parametric model of the migration (Papaloizou and Larwood, 2000; Beaugé et al., 2006; Moore et al., 2013), in which the N-body equations of motion are extended to include additional terms which

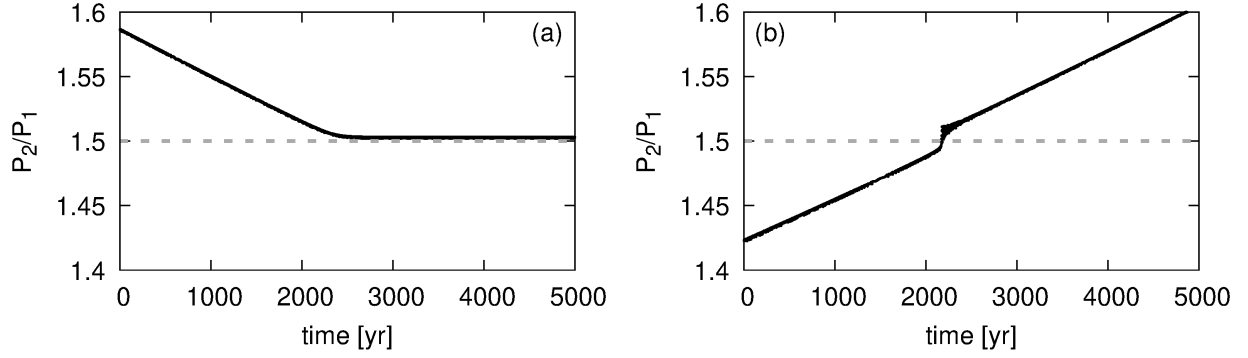


Figure 1: The period ratio evolution of a system of two planets of masses  $m_1 = m_2 = 10 M_\oplus$  around a star of a mass of  $m_0 = 1 M_\odot$  in the cases of convergent (panel a) and divergent (panel b) migration in the vicinity of 3:2 MMR. The initial orbital parameters  $a_1 = 0.2$  AU,  $e_1 = 0.01$ ,  $e_2 = 0$ ,  $\omega_1 = 0$ ,  $\omega_2 = \pi$ ,  $\mathcal{M}_1 = 0$ ,  $\mathcal{M}_2 = 0$  (the same for the two simulations) and  $a_2 = 0.272$  AU (panel a) and  $a_2 = 0.253$  AU (panel b). The migration parameters:  $\kappa = 300$  (for both the simulations) and  $\tau_1 = 1 \times 10^4$  yr,  $\tau_2 = 4 \times 10^3$  yr (panel a);  $\tau_1 = 4 \times 10^3$  yr,  $\tau_2 = 1 \times 10^4$  yr (panel b). The simulation was performed with a help of the parametric model of migration, Eq. 1.

mimic the planet-disc interaction:

$$\mathbf{f}_i = -\frac{\mathbf{v}_i}{2\tau_i} - \frac{\mathbf{v}_i - \mathbf{v}_{c,i}}{\tau_i \kappa_i^{-1}}, \quad (1)$$

where  $\mathbf{v}_i$  is the astrometric velocity of planet  $i$ ,  $\mathbf{v}_{c,i}$  is the Keplerian velocity of a planet in a circular orbit of the size equal to the astrometric distance of the planet. The time-scale of migration of planet  $i$  is denoted with  $\tau_i$ , while the circularisation time-scale of the  $i$ -th planet orbit is given by  $\tau_i$  divided by a constant term  $\kappa_i > 1$ . In the case of non-interacting planets, the model results in the following evolution of the semi-major axes and the eccentricities of planet  $i$  (for  $e_i \ll 1$ ):  $a_i(t) \approx a_i(0) \exp(-t/\tau_i)$  and  $e_i(t) \approx e_i(0) \exp(-\kappa_i t/\tau_i)$ .

In the example shown in the left panel of Fig. 1 the period ratio, which is initially greater than the nominal value of the resonance, decreases until  $P_2/P_1 \approx (p+q)/p$  (here  $p = 2$ ,  $q = 1$ , which corresponds to 3:2 mean motion resonance), after which it starts to oscillate near this value. In the case of the divergent migration (the right panel of Fig. 1) the evolution is different. The period ratio, initially  $< 1.5$ , increases continuously, reaching values  $> 1.5$ . The oscillations of  $P_2/P_1$  around the nominal value do not occur.

In order to understand this effect, one needs to look at the resonance in the context of periodic configurations. Hadjidemetriou (1976) showed that in the planetary  $N$ -body problem (with non-zero planets' masses), in a reference frame co-rotating with one of the planets, there exist families of periodic orbits (configurations) corresponding to mean motion resonances. The evolution of the periodic configuration is such that the system starting from a given point in the phase space (e.g., the space of positions and velocities or the orbital elements), after certain amount of time  $T$  (i.e., the period of the evolution) returns to that point. In other words, the phase trajectory of the system is closed. There exist whole families (branches) of such configurations, parametrised with, e.g., one of the coordinates or, if the state of the system is given by the orbital elements, by the period ratio (the latter parametrisation will be used further in this text). A periodic configuration is represented with a freely chosen point from its trajectory.

Periodic configurations can be stable or unstable. In the former case, if the system (understood as a point in the phase space representing the state of the system) is initially near the closed trajectory, it will be near this trajectory during the evolution. In the latter case, the system will stay in the vicinity of the closed trajectory only for certain finite amount of time.

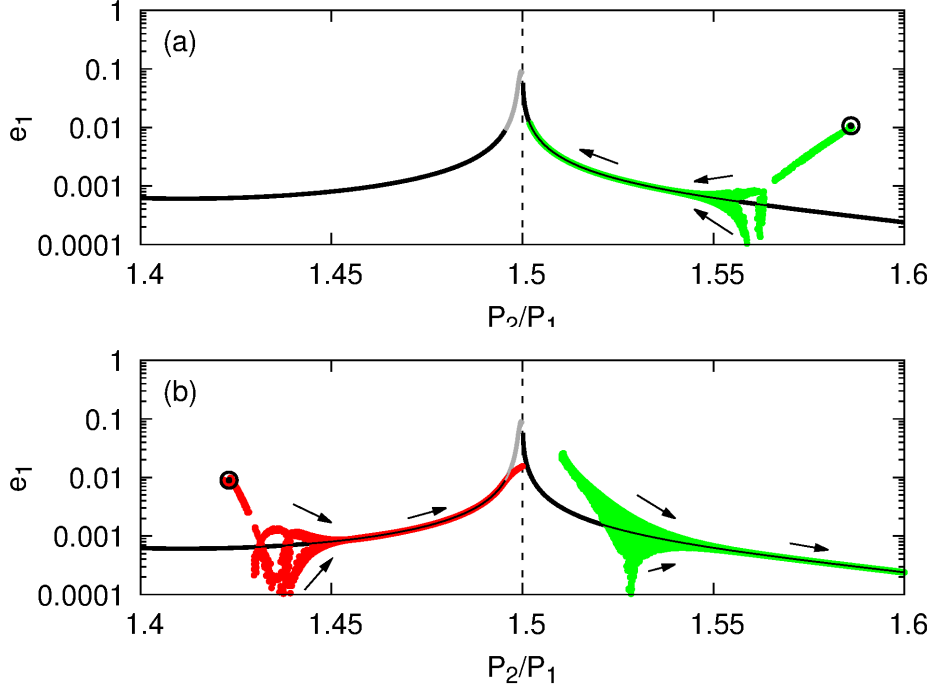


Figure 2: The evolution of the system of two migrating planets presented at the  $(P_2/P_1, e_1)$ -diagram in the case of convergent (panel a) and divergent (panel b) migration. The families of stable and unstable periodic orbits are marked with the black and the grey curves, respectively. The branches for  $P_2/P_1 < 1.5$  correspond to  $\mathcal{M}_1 = 0$  and  $\mathcal{M}_2 = 0$ , while  $\mathcal{M}_1 = 0$  and  $\mathcal{M}_2 = \pi$  for  $P_2/P_1 > 1.5$ . For both the cases  $\Delta\omega = \pi$ . The positions of the system for  $\mathcal{M}_1 \approx 0$  and  $\mathcal{M}_2 \approx 0$  are shown in red, the green colour means that  $\mathcal{M}_1 \approx 0$  and  $\mathcal{M}_2 \approx \pi$ . The arrows show the direction of the evolution. The beginning of the evolution for each simulation is marked with the large black symbol. Panels (a) and (b) correspond to the systems whose evolution was shown in panels (a) and (b) of Fig. 1.

If the planetary migration is slow enough and the planet-disc interaction results in the orbital circularisation (in the typical case), the system of two planets evolves in the phase space along the family of periodic orbits (e.g., Beaugé et al., 2006; Hadjidemetriou and Voyatzis, 2010). Therefore, the periodic configurations are attractors in the phase space for the system with migrating planets. The evolution of the systems presented in Fig. 1 can be also illustrated at the  $(P_2/P_1, e_1)$ -plane together with the families of periodic configurations (Fig. 2).

Figure 2a corresponds to the convergent migration. The period ratio is initially greater than the nominal value of 1.5, i.e.,  $P_2/P_1 \approx 1.586$ , while the eccentricity  $e \approx 0.01$  is significantly different than the value corresponding to the periodic configuration. The migration is convergent, i.e.,  $P_2/P_1$  decreases, simultaneously  $e_1$  decreases in a way that the system (the point in the phase space representing the state of the system) approaches the family of periodic orbits. For  $P_2/P_1 \approx 1.55$  the configuration is already at the branch and evolves further along it, until  $P_2/P_1$  reaches the value close to 1.5 and  $e_1 \approx 0.01$ . The further decrease of  $P_2/P_1$  would result in the increase of  $e_1$ , and for greater  $e_1$ , the circularisation of the orbit is more effective (since  $\dot{e} = -e/\tau_e$ ). The value of  $\approx 0.01$  corresponds to a balance between the excitation of the eccentricity due to the evolution along the branch of periodic orbits and the orbit circularisation due to the planet-disc interaction. It is a typical scenario for the smooth (i.e., without additional perturbations) convergent migration.

In the second case, illustrated in Fig. 2b, the initial  $P_2/P_1 \approx 1.423$  and the migration is divergent. The first part of the evolution of the system at the  $(P_2/P_1, e_1)$ -diagram is shown with the red colour. At

this stage of the evolution the system approaches the family of periodic orbits. For the period ratio of  $\approx 1.45$  the configuration is already at the branch and evolves further along it, until the periodic configurations are no longer stable (the black curve passes into the grey curve). Further evolution (shown with the green colour) does not occur along the branch of periodic configurations, while the period ratio increases up to the values  $> 1.5$ .

Passing between the two branches of periodic orbits is not continuous (e.g., Hadjidemetriou, 1976). For  $P_2/P_1 < 1.5$  the critical argument of the resonance  $\phi_1 \equiv 2\lambda_1 - 3\lambda_2 + \omega_1 = \pi$ , while for  $P_2/P_1 > 1.5$  the resonant angle  $\phi_1 = 0$ . The discontinuity between the two branches results in temporary deviation of the system from the periodic configuration. Besides, during the evolution the system omits the points  $(0, 0)$  and  $(0, \pi)$  at the mean anomalies plane (there are no green points representing the state of the system for  $P_2/P_1 \lesssim 1.51$ ). After certain amount of time the system evolves along the branch of periodic orbits again. Such a situation is typical for the divergent migration. In contrast to the case of convergent migration, there is no equilibrium configuration, i.e., if the time-scales of migration are such that  $\tau_1 < \tau_2$ , the period ratio will increase continuously.

The results presented in articles H1–H5 constituting the scientific achievement will be discussed further in this document. The migration is a key issue in each of the problems studied in the articles, i.e., it is a process which leads to the formation of mean motion resonances and the periodic configurations in particular. In two of the papers, H1 and H5, understanding of the migration mechanism helped to properly interpret the observational data, respectively of the planetary systems around HR 8799 and Kepler-25, as well as to determine the orbital configurations of these two very different (in terms of the masses and linear dimensions) systems. These two papers form a frame of the cycle of the scientific achievement. The three remaining articles, H2–H4, are devoted to the process of the formation of the resonance itself, and do not refer to any particular known planetary system, although the article H4, devoted to the 9:7 MMR formation, was inspired by the previous paper on the Kepler-29 system (Migaszewski et al., 2017).

### **The migration of planets and the problem of finding stable configurations of observed multi-planet systems – the case of HR 8799 (article H1)**

As it was mentioned in the Introduction, in typical situations the migration leads to formation of stable resonant configurations. This fact was used to find the orbital parameters of the HR 8799 planetary system, which correspond to stable evolution and agree with the observations.

The planetary system around HR 8799 was found ten years ago with a help of the direct imaging method. At first, three planets of masses of  $\sim 10$  Jupiter mass ( $M_{\text{Jup}}$ ) were discovered in orbits of periods ranging from  $\sim 100$  to  $\sim 450$  yr (Marois et al., 2008). Two years later the fourth equally massive planet in orbit of  $\sim 50$  yr period was detected (Marois et al., 2010). The system became a target of many studies, one of the goals of which was to determine the orbital configuration of this complex system.

It is not an easy task for two reasons. Firstly, the observations covered initially  $\sim 10$  yr only (it was even less for the innermost planet HR 8799e), what caused the orbital elements determination uncertain. At present, despite additional years of observations, the situation is similar. In other words, the area of the parameter space allowed by the observations is very large – and it is an 18-dimension space, under an assumption that the system is coplanar and the masses are known. Secondly, strong gravitation interactions between the planets and the dynamical compactness of system (the orbital period ratios of subsequent pairs of planets, although known with large uncertainties, are of the order of 2) causes that the parameter space is dominated by strongly chaotic motions. The dynamical compactness is understood here in terms of small semi-major axis/period ratios, i.e.,  $a_{i+1}/a_i$  or  $P_{i+1}/P_i$ , not in terms of small  $a_i$  or  $P_i$ . Because of the linear scalability of the N-body problem, variation of the linear sizes of the orbits results in changing the time-scale of the evolution only, without any changes in the dynamics.

The problems with finding stable configurations in agreement with the observations were reported shortly after the discovery of the first three planets (Fabrycky and Murray-Clay, 2010; Goździewski and Migaszewski, 2009). After the discovery of the fourth one, the situation became even worse. In order to present the problem fully, one needs to mention that the assumption, usually accepted as a necessary condition, that the this relatively young system (the age of the star, however weakly constrained, most likely ranges from  $\sim 30$  to  $\sim 90$  million years; Baines et al., 2012) has to be stable, was abandoned in favour of a hypothesis that the system may self-disrupt in the next few tens of Myr (Goździewski and Migaszewski, 2009). Although, the hypothesis cannot be ruled out a priori, the searching for alternative models was caused by the problems in finding stable configurations, rather than by important astrophysical reasons.

In order to find stable configurations consistent with the observations a following approach is usually used. In the first step, an algorithm of global searching for best-fitting, e.g., in terms of sufficiently low value of  $\chi^2$  function, systems in the parameters space is used, the result of which is a large number of initial conditions. In the second step, the initial conditions are used in the N-body integrations, the purpose of which is to find whether or not a given system is stable. The so called fast chaos indicators are often used to answer this question (e.g., Panichi et al., 2017), as they speed up the stability tests significantly.

In the case of the HR 8799 planetary system, the strategy outlined above was ineffective. As it was mentioned earlier, because of big masses, the dynamical compactness of the system and the short observing window, the probability of finding stable configurations consistent with the observations is very low, of the order of  $\epsilon^{18}$ . The quantity  $\epsilon$  expresses the mean over the parameters of the ratio between a given parameter range corresponding to the stable evolution to the range allowed by the observational constraints. Even for  $\epsilon \sim 0.1$ , the probability of random finding the configuration which is stable and consistent with the observations is of the order of  $10^{-18}$ , while the number of initial conditions which can be effectively tested for stability is  $\sim 10^9$ .

The chances of finding a stable system consistent with the observations can be increased by using other algorithms of the parameters space exploration. In the approach known in the literature as GAMP (Goździewski et al., 2008), the stability is being tested during the process of the fitting the model to the observational data. Nevertheless, because of the large number of parameters and the small area of stable motions, even this improved method fails to reach the goal, without imposing significant limitations on the space of initial conditions.

In both the approaches described above, most (if not whole) of the computational time is used for testing the agreement with the observational and the stability constraints of the configurations which turn out to be unstable. In the approach proposed in H1 only those configurations are being tested in terms of their agreement with the observations of which we know that they are stable. The stability is guaranteed by the process of migration. Nevertheless, the approach requires the assumption of a particular type of the orbital configuration, i.e., resonant, which do not have to be fulfilled (e.g., Götberg et al., 2016).

The approach was described in details in H1, below it will be presented briefly. Within the astrophysical model of the planet-disc interaction the time-scales of migration and circularisation depend on the disc parameters and the planet's mass in a complex way. In the approach presented in H1 the parametric model of migration was used (Eq. 1), in which  $\tau_i$  and  $\kappa_i$  are free parameters. Although the model is simple, it is used here only in order to simulate the process leading to formation of a resonant (i.e., stable) planetary system. As it was explained in the Introduction, the evolution of a system with two migrating planets in the phase space is determined by the structure of periodic orbits, and the latter depends on the number of planets and their masses, while it is independent of

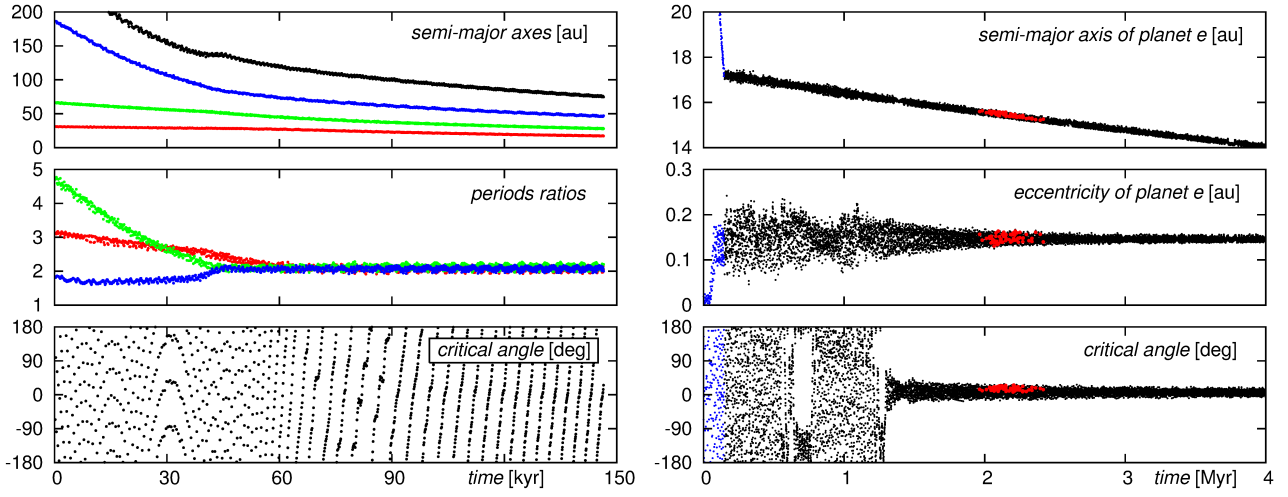


Figure 3: The migration evolution of an example configuration of four planets of masses like in the HR 8799 system presented as time-evolution of the system parameters: the semi-major axes, the period ratios, the critical angle of the chain of resonances 8:4:2:1 ( $\theta = \lambda_1 - 2\lambda_2 - \lambda_3 + 2\lambda_4$ ) and the eccentricity of the innermost planet. The panels on the right correspond to slower migration (see the text for details). The red colour indicate configurations consistent with the observations. The plots were taken from article H1.

the disc parameters or the model of migration. The disc parameters as well as the initial orbits of the HR 8799 system are unknown, and they were not a subject of the studies presented in H1. In other words, in H1 the migration was used as a heuristic method of finding stable resonant configurations, which then were tested whether or not they agree with the observations.

Figure 3, which presents the evolution of an example configuration, is an illustration of the method. The initial orbits are chosen randomly in such a way that the period ratios of subsequent planets  $\geq 2$  and the orbits were wider than presently observed. The migration parameters  $\tau_i, \kappa_i$  (where  $i = 1, 2, 3, 4$  enumerates subsequent planets, starting from the innermost one) were chosen randomly as well, however the choice was such that the migration of each pair of planets were convergent, i.e.,  $\tau_1 > \tau_2 > \tau_3 > \tau_4$ . After  $\sim 60$  kyr of the example evolution the convergent migration leads the period ratios of subsequent pairs of planets to  $P_{i+1}/P_i \approx 2$ , however the critical angle of this chain of resonances,  $\theta \equiv \lambda_1 - 2\lambda_2 - \lambda_3 + 2\lambda_4$ , still rotates (panels in the left column), which means that the system is not yet in the resonance.

When the sizes of the orbits approach the values of the observed system, the migration is being slowed down (panels in the right column). This technical trick is being used in order not to miss configurations consistent with the observations. At each time-step of the integration, the consistency of a given configuration with the observations is tested. In order to verify whether or not the model fits the data, an optimization algorithm is used to find the best-fitting values of the Euler angles, which give the spatial orientation of the system, as well as the best-fitting phase of the N-body evolution of the system (which corresponds to assigning a particular epoch to the initial condition). In the example, after  $\sim 2$  Myr of the migration, the system fits the astrometric data very well. The systems fitting the data are marked with the red colour. At this moment of the evolution the system is already resonant. It is called a four-body resonance. A classical example of such a multi-body resonance known in the Solar system is the three-body Laplace resonance in the system of the Galilean moons: Io, Europa and Ganymede (Sinclair, 1975; Yoder, 1979), in which the subsequent pairs of moons are also involved in two-body 2:1 MMRs.

Figure 4 presents the observational data (the planets positions with respect to the central star) in

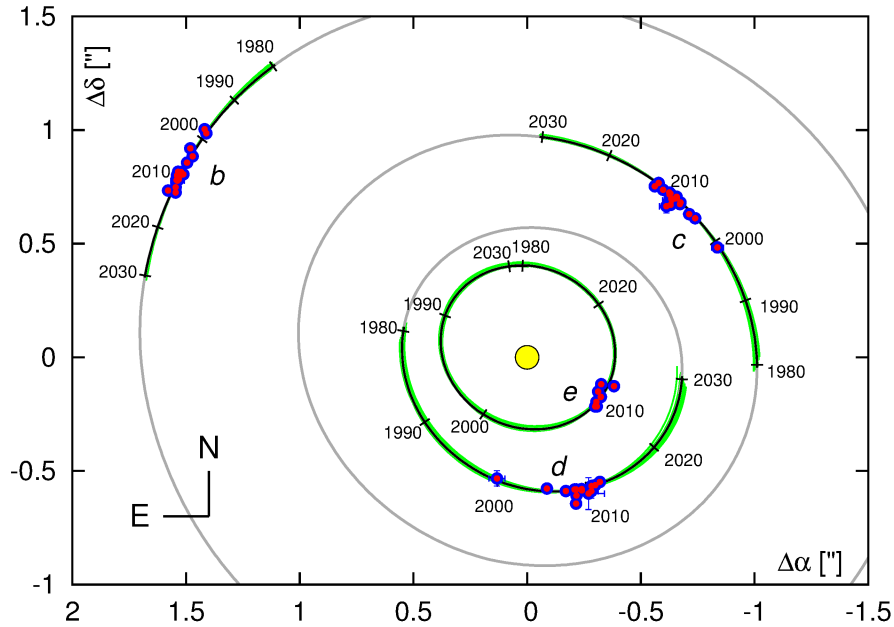


Figure 4: The planets astrometric positions at the sky-plane (red dots) in particular epochs of observations. The star (the yellow disc) is located in the (0,0) point. The green curves illustrate the synthetic orbits (between the epochs of 1980 and 2030) corresponding to stable configurations consistent with the observations. The grey/black curves correspond to the best-fitting systems. The plot was taken from H1.

given epochs with the best-fitting model over-plotted. The model is being used as "the official" configuration of the HR 8799 system in works devoted to studies of the dynamical structure of the dust discs discovered outside the orbit of the outermost planet *b* as well as inside the orbit of the innermost planet *e* (e.g., Contro et al., 2015, 2016; Read et al., 2018). Nevertheless, there are still attempts of finding stable non-resonant configurations (e.g., Götberg et al., 2016). In the recent paper (Goździewski and Migaszewski, 2018), the method proposed in H1 was further improved and used to analyse the extended dataset with new observations. The new analysis confirmed the resonant nature of the system. More results of this work will be described further in this document.

The method presented in H1 was also used to find a good starting point for the photo-dynamical analysis of the Kepler-223 system (Mills et al., 2016). The system, discovered by the KEPLER mission (Borucki et al., 2010, 2011), consists of four planets of masses in a range of a few Earth masses, forming a compact resonant configuration, i.e., the periods of subsequent planets are in ratios of 4:3, 3:2, 4:3. Similarly to the case of HR 8799, the dynamical compactness of the system as well as weak observational constraints (the low signal-to-noise ratio, the relatively narrow observing window) caused that the probability of finding a stable configuration consistent with the observations were very low when the standard approaches of the orbital model optimisation were used. The method proposed in H1 allowed to find such a configuration and confirm the resonant nature of the system.

The article (Mills et al., 2016), published in *Nature* together with American astronomers, were not included in the scientific achievement cycle, because of non-dominant (although important) contribution of the habilitation candidate. Nevertheless, the use of the method presented in H1 in the analysis of a system very different from the one for which the method was invented, as well as for different type of observations, indicate the universality of the approach and the importance of the migration in the process of formation of the orbital configurations of planets' masses as well as the linear sizes from very wide ranges.

## The evolution of two planets in a protoplanetary disc – periodic configurations as final states of the migration (article H2)

As it was shown in the case of HR 8799, the migration plays an important role in formation of the orbital configurations of compact multi-planet systems. It is then natural to study the process more systematically, starting from systems of two planets as well as replacing the parametric model of migration with the astrophysical model. It was the goal of article H2, wherein the study focused on the systems with planets of masses in a few Earth mass regime, and with orbital periods ranging from a few to a few tens of days.

There were two reasons for such a choice. The first one was the fact that thanks to the KEPLER mission (Borucki et al., 2010), there are known hundreds of systems with low-mass, short-period planets, which causes that the results of modelling the migration can be compared with the observed systems, both individually and in a statistical sense. The second reason was that the small planets do not disturb the disc evolution significantly, the result of which is that one can use simplified models of the disc itself as well as the planet-disc interactions, rather than much more time-consuming full hydrodynamical simulations. Such an approach makes it possible to study the evolution of the systems with migrating planets for many different masses and initial orbital parameters.

The direct motivation for the studies presented in H2 was an attempt to explain statistical discrepancies between the histogram of the period ratios resulting from the migration simulations and the one for the known systems, discovered mainly by the KEPLER mission (Fabrycky et al., 2014). It turns out that the number of systems whose period ratios are close to resonant values of  $2/1, 3/2, 4/3$ , etc., is not big, i.e., in the histogram of  $P_2/P_1$  for the observed systems there are no significant maxima around the resonant values (apart from a weak maximum around the 3:2 MMR).

If the convergent migration was a leading mechanism, the maxima in the histogram should be very strong and vast majority of the systems should have  $P_2/P_1 \approx (p + 1)/p$ , because of the dominant role of the first order MMRs. On the other hand, if the planets migrated mainly divergently, the configurations would not be so compact, i.e., most of the systems would be hierarchical with  $P_2/P_1 \gtrsim 10$ .

There are several explanations of the discrepancy proposed in the literature. Among them there are the disc turbulences (Nelson, 2005) or the interactions between the planets and the planetesimals which left in the system after the disc dispersal (Chatterjee and Ford, 2015). Another proposed mechanism is the divergent migration caused by the tidal interactions between the planets and the central star (Papaloizou, 2011; Batygin and Morbidelli, 2013; Delisle and Laskar, 2014).

It was proposed in H2 that the discrepancy mentioned above could be explained by alternate convergent and divergent migration which results from the complex disc structure as well as its evolution. The so called  $\alpha$ -disc model was constructed (e.g., Shakura and Sunyaev, 1973), i.e., the model in which the turbulent viscosity is treated in a simplified way. The disc parameters, i.e., the accretion rate, determined with the value of  $\alpha$ , as well as the photo-evaporation rate (Matsuyama et al., 2003), were chosen such that the disc exists long enough, so the planets of a few Earth masses, starting from the orbits of sizes of  $\sim 1$  AU migrate inwards down to the orbital periods ranging from a few up to a few tens of days. It was shown in this paper that in order to obtain a realistic disc model it was necessary to account for the opacity dependence on the temperature and density of the disc of gas and dust (the opacity tables from Semenov et al., 2003, were used).

When at a given time and the astrocentric distance the physical disc parameters are known, the disc-induced force acting on the planet is being computed with a help of approximated formulae, mainly from (Paardekooper et al., 2011; Tanaka and Ward, 2004), governing the migration and the circularisation of low-mass planets. The transition into the range of more massive planets was also accounted

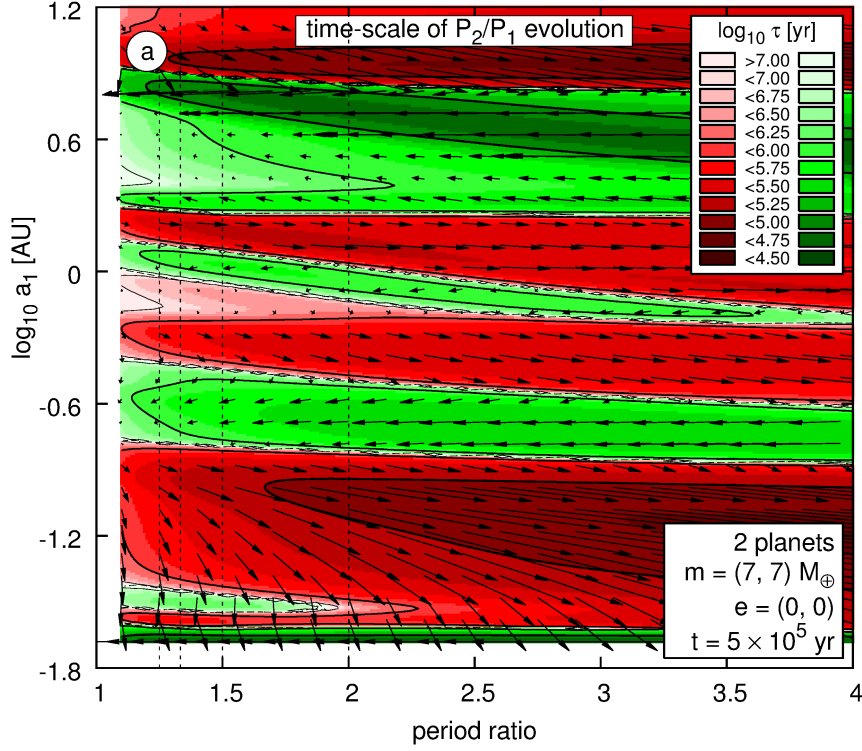


Figure 5: The colour palette illustrates the time-scale of the  $P_2/P_1$  variation as a function of  $(P_2/P_1, a_1)$ . The green colour denotes the convergent migration, the red colour – divergent. The stronger the colour is, the faster is the evolution of the period ratio. The arrows form a vector field of a system of two planets at the  $(P_2/P_1, a_1)$ -diagram. The plot corresponds to the planets’ masses of  $m_1 = m_2 = 7 M_\oplus$  and a given epoch of the evolution of the disc ( $t = 5 \times 10^5$  yr). The plot was taken from H2.

for (Dittkrist et al., 2014). The force computed in this way is being added to the N-body equations of motion, which are being integrated numerically for the time-interval of  $\sim 3$  Myr, corresponding to the disc life-time. The disc model is described in details in H2.

One of the goals of the paper was to illustrate that for different astrocentric distances the planetary migration may occur in different time-scales, in particular changing its direction. As a consequence the migration of a given pair of planets may be convergent or divergent, depending on their positions in the disc. In general, the period ratio may increase or decrease alternately. Besides that, the disc itself evolves, which makes the regions of convergent and divergent migration move towards the star. The combination of these two effects causes that the final result (i.e., the period ratio) may be difficult to predict without following the evolution during the whole life-time of the disc.

Figure 5 presents the regions of convergent and divergent migration of planets of equal masses of  $m_1 = m_2 = 7 M_\oplus$  in a given epoch of the disc evolution. The arrows form the vector field at the  $(P_2/P_1, a_1)$ -diagram. In general, the evolution of the system at the diagram, which varies during the disc evolution, is very complex. In particular, the inner part of the disc corresponds to the divergent migration.

A number of 3500 migration simulations for randomly chosen planets’ masses and initial orbits were performed and presented in H2. The final result was negative in terms of explaining the discrepancy between the observed and synthetic period ratios histograms, however the resulting systems are characterized with  $P_2/P_1$  from the whole range of values. Among the final systems there were very compact configurations with  $P_2/P_1 \approx 1.2$  as well as ones with  $P_2/P_1 \gtrsim 2$ , including hierarchical systems whose  $P_2/P_1 \sim 10$ .

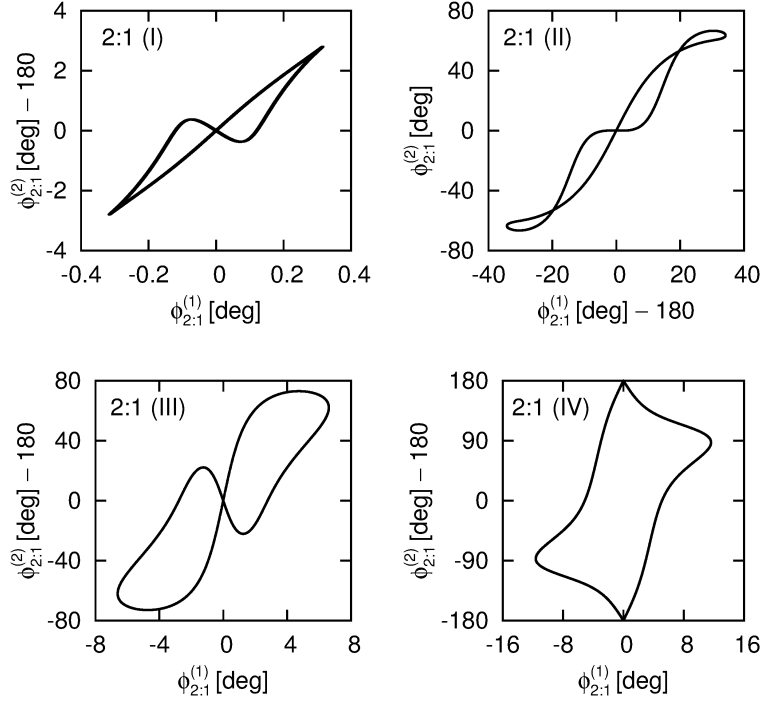


Figure 6: The evolution of four example systems, which are results of the migration simulations in the evolving disc, presented at the diagrams of resonant angles  $\phi_{2:1}^{(1)} \equiv \lambda_1 - 2\lambda_2 + \omega_1$  and  $\phi_{2:1}^{(2)} \equiv \lambda_1 - 2\lambda_2 + \omega_2$ . The integration time of the N-body equations of motion is  $10^5 P_2$ . The plots were taken from H2.

The negative result was caused by the fact that the agreement between the synthetic and the observational statistics of the systems depend strongly on the assumed distribution of the planets' masses. If for most of the systems  $m_1 \gtrsim m_2$ , the  $P_2/P_1$  histogram lacks of significant maxima around the resonant values, for the opposite case there are strong maxima, which get stronger when more systems have  $m_1 \lesssim m_2$ . The planets' masses of significant fraction of the observed systems are known poorly. In particular, expected amplitudes of the transit timing variation (TTV) are below the measurements uncertainties for configurations whose  $P_2/P_1$  are far from the nominal resonant values. Moreover, the final  $P_2/P_1$  distribution depends on the distribution of initial orbits, which are unknown. Therefore, testing the agreement between the period ratio distribution of the synthetic systems with the one of the observed configurations may be unreliable.

Nevertheless, the study described in H2 resulted in finding a common feature of the systems of different  $P_2/P_1$  values, which is independent of the issues mentioned above. Almost all the systems resulting from the migration turned out to be periodic configurations. Figure 6 illustrates the evolution of four example systems at the diagram of the critical angles of the 2:1 resonance. The system I (the top-left panel) corresponds to the period ratio greater than 2, but very close to the nominal value. The systems II and III have  $P_2/P_1$  shifted slightly with respect to 2, i.e.,  $P_2/P_1 \sim 1.95$  (II) and  $P_2/P_1 \sim 2.05$  (III). The system IV has  $P_2/P_1 \gtrsim 2.12$ .

The phase trajectories of these systems are closed (the plots present projections of the trajectories at the plane of chosen parameters). Almost all the systems resulting from migration evolve in this way. The exceptions are the hierarchical systems with high value of  $P_2/P_1$  and some of the configurations involved in higher-order resonances. The latter will be explained in H4.

As it was mentioned in the Introduction, the correspondence between the migration and the periodic orbits have been discussed in the literature (e.g., Ferraz-Mello et al., 2003; Beaugé et al., 2006; Hadjidemetriou and Voyatzis, 2010). In H2 it was also shown that the exact periodic configurations are

final states of the migration. The article H5 presents an attempt of showing that the observed systems may be in fact periodic configurations. The closeness of a given system to the periodic configuration indicates that the migration was smooth (i.e., slow and without additional perturbations caused by the disc turbulences or the planetesimals). Before describing the results of that work, in the next section the results of the studies of the migration of three planets will be presented (article H3), as they bring an additional characteristic of the systems, which could be used to put constraints on the migration parameters.

### **The evolution of three planets in a protoplanetary disc – chains of mean motion resonances (article H3)**

The article H3 presents the results of analogical simulations as in H2, but devoted to three-planet systems. Similarly to the case of two planets, the migration of subsequent pairs of planets in the three-planet systems can be convergent or divergent, depending on the planets' positions in the disc and well as the evolution stage of the disc itself. Because of a greater number of the orbital parameters, the structure of the periodic orbits, and as a result the evolution of the three-planet systems, is more complex than in the problem discussed in H2.

Similarly to the case of the two-planet systems, in which the migration leads to formation of mean motions resonances, the so called chains of mean motion resonances may be the final results of the migration of three planets, an example of which is the four-planet system around HR 8799 discussed earlier. In such a case, subsequent pairs of planets are involved in mean motions resonances, i.e., their resonant angles librate. As a result, the system of three planets as a whole is involved in a three-body resonance.

The evolution of an example system of three planets is shown in Fig. 7 (the left panel) as an evolutionary path at the diagram of the period ratios. The system starts from the point marked with 0. Initially, the migration of both the pairs of planets is convergent and the period ratios  $P_2/P_1$  and  $P_3/P_2$  decrease down to the nominal values of the 3:2 and 4:3 resonances (the point marked with 1 at the diagram), which leads to the resonant synchronisation of the system (the chain of resonances is formed). Because of the change of the planets' positions in the disc as well as the change of the disc itself, the migration becomes divergent and the period ratios  $P_2/P_1$  and  $P_3/P_2$  increase – the evolutionary path passes through points 2 and 3; the evolution direction is shown with the arrow. After reaching the point of coordinates ( $\sim 5/3, \sim 3/2$ ), which corresponds to the chain of 5:3 and 3:2 resonances, further evolution occurs along the horizontal line until the point ( $\sim 2/1, \sim 3/2$ ), marked with 4. After passing through this point, the system continues the divergent migration (both the period ratios increase), until reaching point 5, after which the system turns back to point 6. The final result of this complex evolution is a periodic configuration, which corresponds to the chain of 2:1 and 3:2 MMRs. Therefore, the phase trajectory of this configuration is closed, what can be seen in the right panel of Fig. 7 as a projection at the diagram of the differences of the longitudes of pericentres.

The results of 2700 simulations performed for various planets' masses and the initial orbits are illustrated in the left panel of Fig. 8. The black points indicate the positions of the synthetic systems at the diagram of the period ratios after the disc dispersal. Majority of the points are placed along the grey curves. The curves correspond to the evolution path of the system illustrated in Fig. 7, more precisely the fragments of the paths determined by the points 1, 2, 3 as well as 4, 5, 6.

In the case of divergent migration and under the assumption that the system stays in the resonance, the period ratios  $x \equiv P_2/P_1$  and  $y \equiv P_3/P_2$  vary in a strictly defined way. For the chain of first-order resonances,  $x \approx (q + 1)/q$  and  $y \approx (p + 1)/p$ , the critical angle of the three-body resonance  $\theta \equiv q\lambda_1 -$

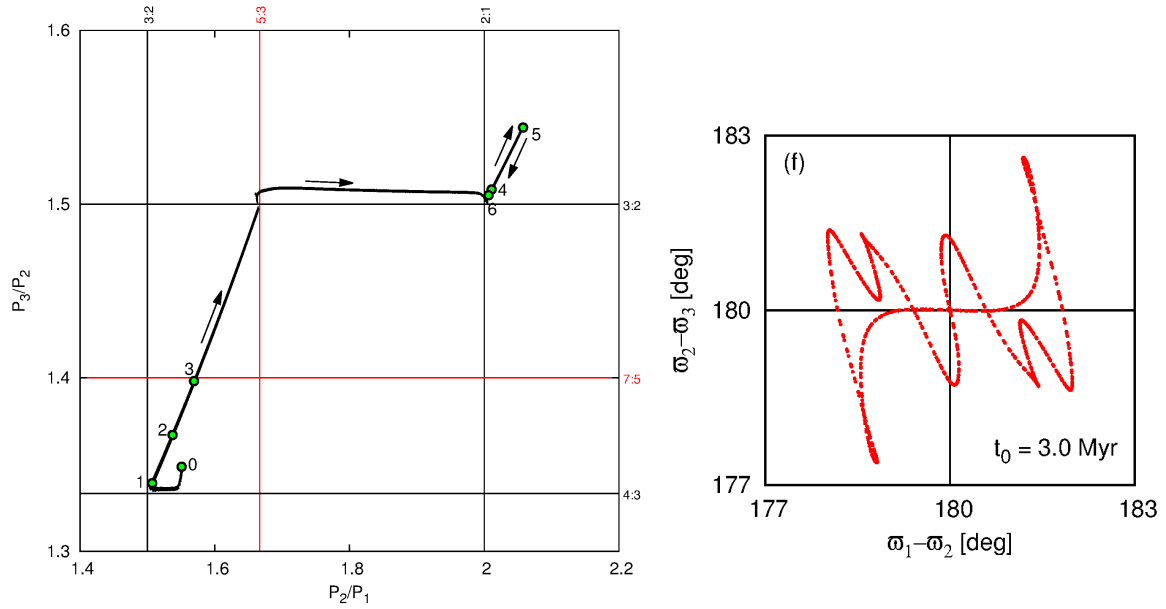


Figure 7: On the left: The evolution of an example system at the period ratios diagram. The evolution direction is shown with the arrows. Subsequent stages of the evolution are enumerated from 0 (the beginning of the simulation) up to 6 (the end of the simulation). The horizontal and vertical lines denote the resonant values. On the right: The N-body evolution of the system after the disc dispersal, illustrated at the  $(\Delta\omega_{1,2}, \Delta\omega_{2,3})$ -diagram. The plots were taken from H3.

$(q + p + 1)\lambda_2 + (p + 1)\lambda_3$ . If the angle librates, the period ratios  $x$  and  $y$  are related in a following way:

$$\frac{1}{y} = 1 + \frac{q}{p+1} (1 - x). \quad (2)$$

The equation defines the evolutionary path of a resonant three-planet configuration migrating divergently. It means that the system which got synchronised in the resonance, remains resonant in a sense of librating critical angles, even though its further migration is divergent, which results in an increase of the period ratios with respect to the nominal values of  $(q + 1)/q$  and  $(p + 1)/p$ .

In a general case of the divergent migration of three planets  $\tau_1 < \tau_2 < \tau_3$ , i.e., without the three-body resonance, the period ratio of each pair of planets evolve independently –  $x$  and  $y$  increases according to formulae  $\dot{x} = 1.5 x (\tau_1^{-1} - \tau_2^{-1})$  and  $\dot{y} = 1.5 y (\tau_2^{-1} - \tau_3^{-1})$  – therefore,  $x, y$  do not have to vary according to  $y(x)$  given by Eq. 2, which corresponds to the resonant evolution. The location of a given configuration at such a curve indicates the formation scenario described above.

The left panel of Fig. 8 shows, apart from the synthetic systems mentioned above (the black points), the positions of known three-planet systems discovered by the KEPLER mission (the green points) within the period ratios range of  $\lesssim 1.8$ . The comparison of the distributions of the black and green points leads to the conclusion that the known systems do not obey the predicted distribution at the period ratio diagram.

In order to explain the discrepancy, a series of simulations within the parametric model of migration were performed (Eq. 1; the right panel of Fig. 8). The migration is initially convergent, which results in the resonant synchronisation of the system (the  $\theta$  angle librates). Next, the migration becomes divergent. The deviation from the nominal values of  $x = 5/4, y = 4/3$  occurs along the curve described above (the dashed line) if  $\kappa$  is sufficiently high, while already for  $\kappa \gtrsim 25$ , obtaining a configuration similar to Kepler-431 cannot be achieved within the scenario presented here (the divergent migration from the three-body resonance). Only for lower values of  $\kappa \lesssim 20$ , it is possible that the system becomes non-resonant and the period ratios  $x$  and  $y$  vary independently.

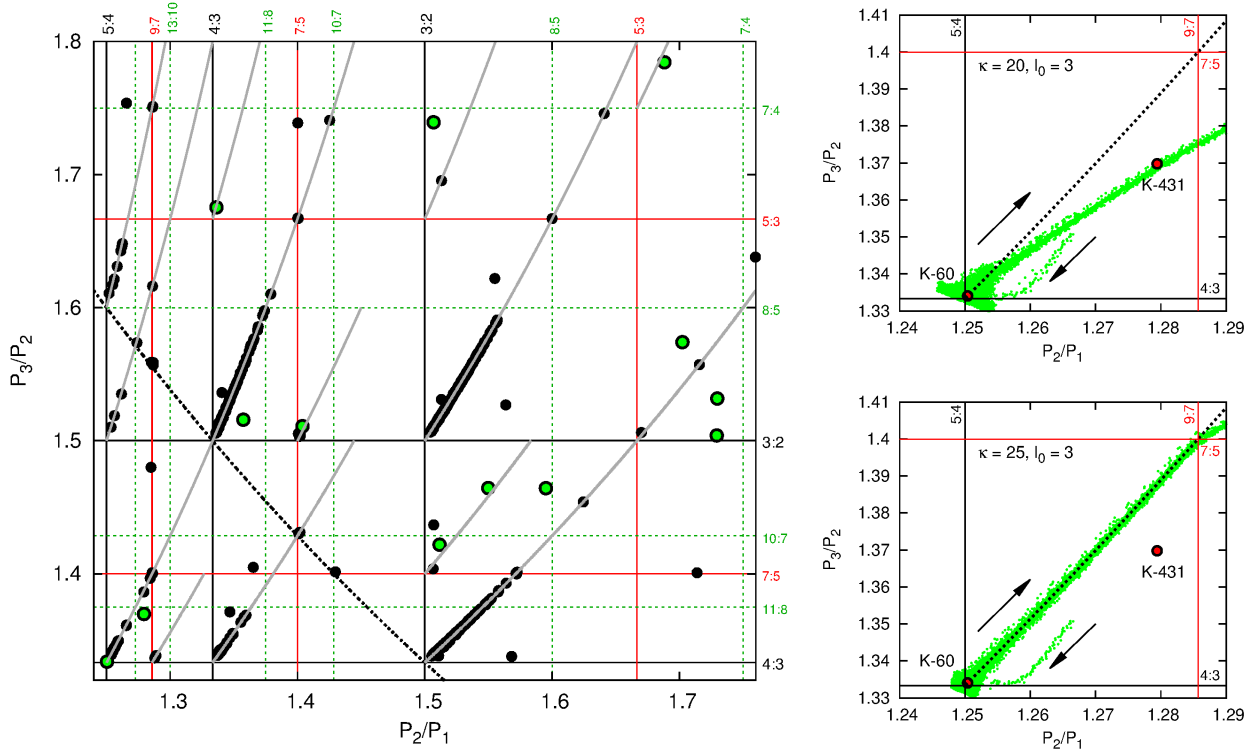


Figure 8: On the left: The statistics of the synthetic systems resulting from the simulations (the black points) and of the known systems (the green points), together with the evolutionary paths of resonant configurations (the grey curves). On the right: The evolution of three-planet systems within the parametric model of migration (Eq. 1), under an assumption that the migration which is initially convergent, changes to divergent after 5 Myr. The two simulations differ one from the other with the value of the  $\kappa$  parameter only. The direction of the evolution is shown with the arrows. The dashed line denotes the evolutionary path of the system in the 5:4, 4:3 chain of resonance. The red points indicate the positions of two known three-planet systems, Kepler-60 and Kepler-431. The plots were taken from H3.

The astrophysical model described in articles H2 and H3 make use of analytic formulae for  $\tau_a$  and  $\tau_e$ , which are functions of the disc and planet parameters. The values of  $\kappa$  stemming from the model are very high  $\sim 1000$ , which probably results from the too simple physical model of the disc and its interaction with a planet in an elliptic orbit (Tanaka and Ward, 2004). In fact, the circularisation rate (and the value of  $\kappa$  as a result) is not well known. For low mass planets it is likely that  $\kappa \sim 30$  (Kley et al., 2009), however in other papers (e.g., Papaloizou and Larwood, 2000; Cresswell and Nelson, 2006) the hydrodynamical simulations lead to circularisation rates even higher than in (Tanaka and Ward, 2004). The problem of estimating the value of  $\kappa$  is still open.

Therefore, a relatively low value of  $\kappa$  is one of possible conclusions stemming from the comparison between the results of the simulations and the statistics of the observed configurations. Nevertheless, if the scenario of the divergent migration of a system in resonance was incorrect, the above reasoning would not be justified. In fact, the observed systems could have never been in resonance. Another possible explanation of the discrepancy discussed here is that the migration is not "smooth", i.e., that one cannot neglect the disc turbulences and/or the planets' interactions with the planetesimals left after the disc dispersal. Although the problem remains unresolved, the period ratio distribution at the  $(P_2/P_1, P_3/P_2)$ -diagram provides additional informations with respect to what one can infer from the period ratio histogram alone.

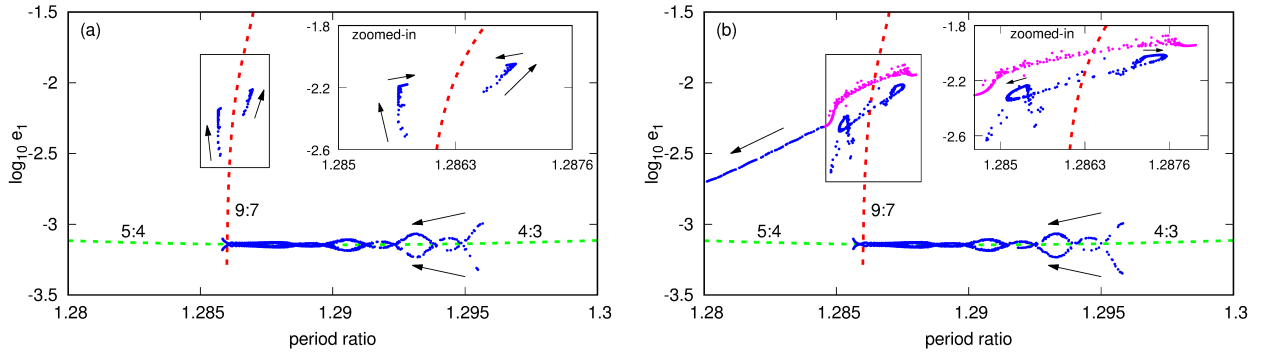


Figure 9: The evolution of an example system with two planets migrating convergently, for the initial  $P_2/P_1 \gtrsim 9/7$ . The positions of the system at the diagrams are shown with blue and pink colours (for  $\mathcal{M}_1 \approx \pi$ ,  $\mathcal{M}_2 \approx \pi$ ) plotted over the branches of periodic orbits (the dashed curves: green for the first-order resonances 4:3 and 5:4 and red for the 9:7 MMR). The families of periodic configurations correspond to  $\mathcal{M}_1 = \mathcal{M}_2 = \pi$ . The direction of the evolution is shown with the arrows. The fragments of the evolution in 9:7 MMR are shown in zoom. The planets' masses  $m_1 = m_2 = 6 M_\oplus$ , the mass of the star equals the Solar mass. Panels (a) and (b) correspond to almost identical initial conditions (see the text for details). The plots were taken from H4.

#### The formation of the second order resonances on an example of 9:7 mean motion resonance (article H4)

As it was demonstrated in the two articles described above, the first order mean motion resonances play an important role in the formation of the orbital configurations as results of planetary migration in protoplanetary discs. Nevertheless, the migration can lead to the formation of higher order resonances as well. It is more difficult, though, because of the structure of periodic orbits related to such resonances. The second and higher order resonances as well as the chains of resonances of this sort were among the results of the simulations presented in H2 and H3, however such configurations were rare, constituting a few per cent of the sample.

The TTV analysis of the Kepler-29 system presented in (Migaszewski et al., 2017) showed that the system is likely involved in 9:7 MMR. This result was the motivation of a systematic study of the process of formation of such a configuration as an example of the second order resonance, which was the goal of article H4. The parametric model of migration, Eq. 1, was used in the study.

The process of formation of the first order resonance (on the example of 3:2 MMR) was discussed in the Introduction and illustrated in the top panel of Fig. 2. The family of periodic orbits (the branch for  $P_2/P_1 > 1.5$ ) occupies a wide range of the period ratio and the eccentricity varies slowly with the change of  $P_2/P_1$ . Because of that, the system parameters vary relatively gradually.

The situation is different in the case of the second order resonance. Figure 9 presents the families of periodic orbits of the first order MMR (4:3 and 5:4; the green dashed curve) and the 9:7 resonance (the red dashed curve). The blue and the pink dots denote the positions of the system at the  $(P_2/P_1, a_1)$ -diagram in moments of time, when both the mean anomalies are close to  $\pi$ .

The branches of periodic orbits are represented by the positions of the configurations at the  $(P_2/P_1, e_1)$ -diagram for fixed phases, i.e.,  $\mathcal{M}_1 = \mathcal{M}_2 = \pi$ . The initial conditions of the two simulations differ slightly one from the other by the value of  $a_2$ , i.e.,  $a_2 = 0.11874$  AU (panel a) and  $a_2 = 0.11875$  AU (panel b). The remaining orbital parameters as well as the planets' masses and the migration parameters are the same in both the simulations.

The first part of the evolution is almost identical for both the systems. The period ratio decreases down

to the nominal value of the 9:7 resonance. Until this moment, the system evolves along the family of periodic orbits of the 4:3 MMR. The branch of periodic configurations of the 9:7 resonance is almost perpendicular to it. The further evolution occurs along the red curve, i.e., the period ratio does not change significantly, while the eccentricities grow up to their equilibrium values.

The difference between the two cases is visible from this point. In the situation presented in panel (a), the system (more precisely: the point in the phase space representing the state of the system) approaches the periodic configuration, while in the second case (panel b), the system deviates from it, and after certain amount of time it evolves towards the branch of periodic orbits of 5:4 MMR.

In the first case, the entrance into the resonance<sup>1</sup> is permanent (or stable), since the system evolves towards the periodic configuration, although because of the finite amount of time (finite life-time of the disc), the final state of the system may differ from periodic.

In order to better illustrate the behaviour of the system after entering the resonance, the averaged model of the resonant system was used (Michtchenko and Ferraz-Mello, 2001; Beaugé et al., 2003). The procedure of the averaging of the Hamiltonian of the system over the so called fast variables (here, the mean anomalies) results in the reduction of the number of the degrees of freedom as well as the elimination of the fast variability, i.e., the evolution in time-scales of the order of the orbital periods. The equilibrium of the averaged system is a counterpart of the periodic configuration in the full, unaveraged, model. A family of equilibria in the averaged model correspond to a family of periodic orbits.

Figure 10 presents the evolution of four chosen initial configurations (points I, II, III and IV), each of which was initially in 9:7 MMR. The evolution is illustrated at the so called representative plane of initial conditions, i.e., the plane of the eccentricities corresponding to fixed values of the total angular momentum  $C$  and the so called scaling parameter  $K$  (Michtchenko and Ferraz-Mello, 2001; Beaugé et al., 2003). The semi-major axes are then functions of the eccentricities and the integrals  $C$  and  $K$ . Additionally, the resonant angles  $\sigma_i \equiv (1 + s)\lambda_2 - s\lambda_1 - \omega_i$ ,  $i = 1, 2$ , where  $s = p/q = 7/2$  are fixed, i.e.,  $(\sigma_1, \sigma_2) = (\pi/2, \pi/2)$  or  $(\sigma_1, \sigma_2) = (\pi/2, -\pi/2)$ .

The point in the centre of the plot (the intersection of the two green curves) denotes the equilibrium of the system of given values of the integrals  $C$  and  $K$ , which corresponds to the periodic configuration of the unaveraged model. The green curves denote the stable periodic configurations of the averaged system (the red curves correspond to the unstable configurations). The evolution of the periodic configuration of the averaged system occurs, analogically to the case of the full model, along a closed phase trajectory, with this difference that the phase space is reduced due to the elimination of the fast variability. For given values of  $C$  and  $K$  there exist families of periodic orbits parametrised by the energy integral. Since, after the averaging, the mean system has two degrees of freedom, the periodic configuration is represented at the Poincaré cross section with a fixed point.

After adding the migration terms to the averaged equations of motion, one can follow the evolution of a given system at the representative plane (the black curves). The evolution of each initial system occurs in the first phase parallel to the vertical branch of the periodic orbits, while after reaching the horizontal branch, the system evolves along it, either towards the equilibrium or away from it.

The system marked at the diagram with I starts furthest away from the equilibrium, a result of which is that the configuration deviates from the resonance centre, and, as a consequence (what is not shown here), the system leaves the resonance. The dynamical area of the resonance is bordered with a separatrix – the grey points (in fact, the resonance has a complex structure). The remaining configurations

---

<sup>1</sup>The entrance of the system into the resonance is understood as a change of the position of the point in the phase space representing its state from the non-resonant region to the resonant part of the phase space. Analogically, the system may leave the resonance.

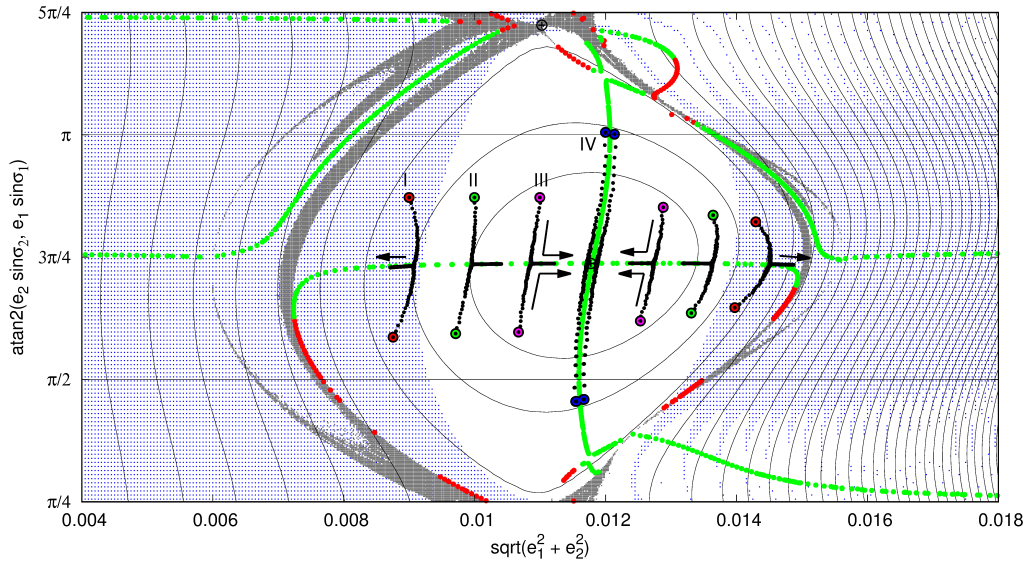


Figure 10: The representative plane of  $(e_1, e_2, \sigma_1, \sigma_2)$  for  $(\sigma_1, \sigma_2) = (\pi/2, \pm\pi/2)$  presenting the energy levels of the averaged system near the 9:7 MMR (the black thin curves), the stable and unstable periodic configurations (respectively, the green and the red curves). The stable equilibrium is determined by the crossing of two green curves in the centre of the diagram. The evolution of example systems with two planets migrating convergently are given by black curves. The blue dots correspond to the initial configurations, which end the simulations as non-resonant systems. The grey colour denotes the chaotic evolution. The plot was taken from H4.

II, III and IV evolve towards the equilibrium, therefore they stay in the resonance. The blue points denote the initial configurations which leave the resonance during the migration, therefore the white area denotes the convergence zone of the resonance.

As it was shown in Figs. 9 and 10, the decisive factor in the resonance formation is the distance of the system from the periodic configuration (or the equilibrium within the averaged model) directly after entering the resonance. If the distance is too big, the system will leave the resonance. The existence and size of the convergence zone depend on the planets' masses. In particular, it is possible that the permanent resonance cannot be achieved in a certain mass range (Xu and Lai, 2017). It was shown in H4 that the existence of such a zone depends also on the equilibrium values of the eccentricities as well as on the dependence of the migration rate on the astrocetric distance of a planet.

#### The periodic configurations of the observed planetary systems – the case of Kepler-25 (article H5)

It was shown in H2 and H3 that the smooth migration in the systems of two and three planets results in the periodic configurations. That refers mainly to the first order resonances or chains of such resonances, however, as demonstrated in H4, systems in the second order MMRs can be close-to-periodic as well. Therefore, the periodic orbits may be a characteristic feature of the systems formed on the way of smooth migration. A natural question arises whether the feature can be verified by observations.

Determination of the frequency of periodic or close-to-periodic configurations among the known systems with two or more planets could help to estimate ranges of the migrations parameters as well as indicate how important were the disc turbulences or the planets' interactions with planetesimals at the early stages of the planetary systems formation. In H5 an attempt was made to determine if a given system is a periodic configuration.

A system of two planets around Kepler-25 (Steffen et al., 2012) was chosen for the analysis, the period ratio of which  $P_2/P_1 \approx 2.039$ , i.e., the system is close to the 2:1 MMR. A relatively good signal-to-noise

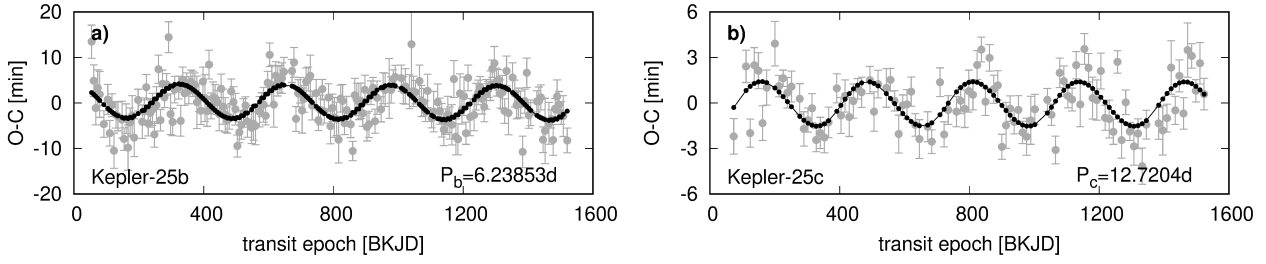


Figure 11: The transit timing variation (TTV) of the Kepler-25 system (the grey points with the error bars) and the model values for the periodic configuration (the black points). The plots were taken from H5.

ratio of the TTV as well as the observing window encompassing a few periods of the TTV modulations were the reasons of that choice. In the group of the systems discovered by the KEPLER mission only few fulfil both the criteria given above, the reason of which will be explained below.

As it was mentioned, a resonant system which is described with the averaged Hamiltonian, can be in an equilibrium, which is a counterpart of a periodic configuration of a system characterised by the full Hamiltonian (i.e., unaveraged). The evolution of the system in the equilibrium means, in particular, that the semi-major axes, eccentricities, as well as the angles  $\Delta\omega \equiv \omega_1 - \omega_2$  and, for the 2:1 MMR,  $\phi_1 \equiv \lambda_1 - 2\lambda_2 + \omega_1$  (the second resonant angle  $\phi_2 \equiv \lambda_1 - 2\lambda_2 + \omega_2 = \phi_1 + \Delta\omega$ ) are constant. The constancy of  $\phi_1$  and  $\Delta\omega$  (as well as  $a_i, e_i$ ) together with the fact that  $\dot{\lambda}_i \approx n_i$  for  $|\dot{\omega}_i| \ll n_i (i = 1, 2)$ , causes that the orbits of the system in equilibrium rotate uniformly with a period of  $T_{(O-C)} = P_2/|2-x|$ , where  $x \equiv P_2/P_1$ , while their apsidal lines are anti-aligned ( $\Delta\omega = \pi$ ). The period is called the super-period in the literature (Lithwick et al., 2012).

The apsidal lines rotations, when the remaining orbital parameters are constant, result in the transit timing variations with respect to the equidistant transit times of the unperturbed Keplerian motion. That stems from the fact that the orbital motion in an elliptic orbit is uneven, the effect is stronger for higher eccentricities. The variability of the transit times occurs with a period  $T_{(O-C)}$ , while the amplitude with respect to the orbital period is proportional to the eccentricity.

For the Kepler-25 system  $x \approx 2.039$ , which leads, under the assumption of the periodic configuration, to  $T_{(O-C)} \approx 325$  d, i.e., the value in agreement with the observations. Since the TTV amplitudes depend on the eccentricities, which in turn depend on the planets' masses and the period ratio, it is possible to determine the latter, i.e.,  $m_1 = (10.8 \pm 1.1) M_\oplus$  and  $m_2 = (14.5 \pm 1.3) M_\oplus$ . The observational data are presented in Fig. 11 together with the model corresponding to the periodic configuration.

As it was mentioned above, the sample of the systems discovered with a help of the transits method contains only few systems with the TTV signals of both high amplitudes and short periodicity with respect to the observing window of  $\sim 1500$  d. The amplitudes increase with a proximity of  $P_2/P_1$  to the nominal value. On the other hand, the proximity results in an increase of  $T_{(O-C)}$ . Therefore, the systems with  $P_2/P_1 \cong (p+q)/p$  have usually too long period  $T_{(O-C)}$  in order to observe the transit timing variations within the observing window of  $\sim 1500$  d. The TTV signals of the systems with  $P_2/P_1$  too distant from the nominal value have very small amplitudes. Naturally, for more massive planets the situation would be better, nevertheless majority of the systems discovered by the KEPLER mission consist of small planets of masses in the range of a few Earth masses.

Finding the periodic configuration which fits the TTV data of the Kepler-25 system does not mean, though, that the system represents the configuration of this sort. Similarly to the case of HR 8799 (article H1), it is only an assumption, whose consistency with the observations was demonstrated. In the case of HR 8799 the stability of the resonant system, in contrast with unstable non-resonant

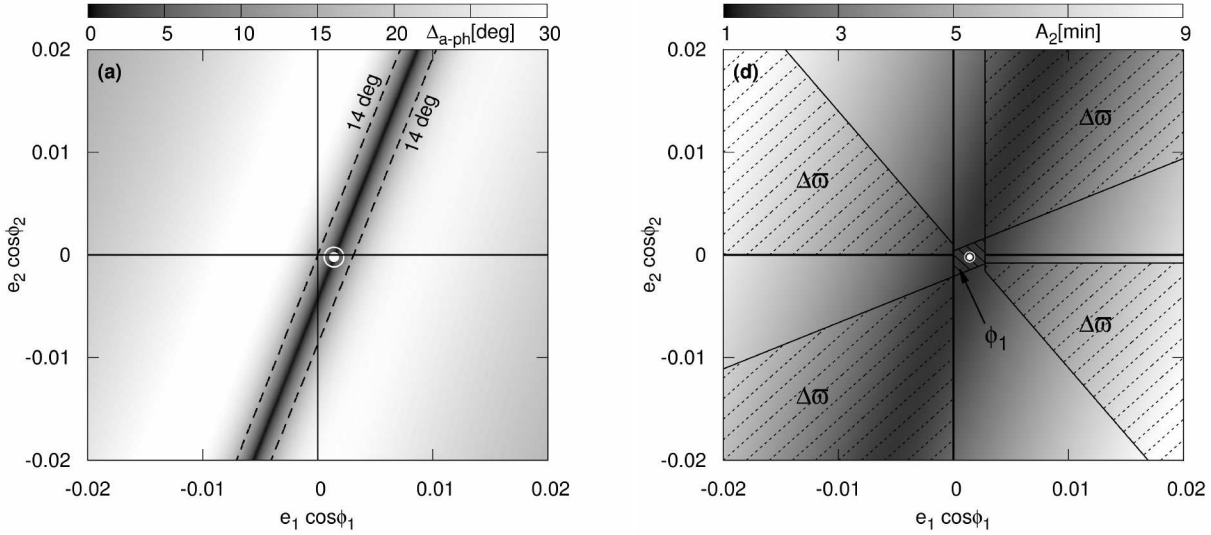


Figure 12: On the left: The difference (with respect to 180 degrees) of the synthetic TTV signals phases presented at the  $(e_1 \cos \phi_1, e_2 \cos \phi_2)$ -plane. The white point denote the periodic configuration corresponding to the best-fitting system. On the right: The amplitude of the TTV signal of the outer planet. The cross-hatch areas correspond to the oscillations of  $\Delta\omega$  and  $\phi_1$ . The plots were taken from H5.

systems, was an additional point for the assumption. The Kepler-25 system of two low-mass planets is stable regardless the resonant synchronisation, which results from the fact that  $P_2/P_1$  is sufficiently distant from the nominal value.

It is therefore natural to ask, whether configurations other than periodic could fit the observations as well. Or differently, would it be possible to find out if the system is periodic with a help of the standard TTV analysis. In order to answer these questions, the TTV characteristics (the period, amplitudes and the difference of phases) were computed as functions of the eccentricities as well as the angles  $\phi_1, \phi_2$ , wherein the values of the angles were limited to their representative values (Beaugé et al., 2003), i.e.,  $(\phi_1, \phi_2) \in \{(0, 0), (0, \pi), (\pi, 0), (\pi, \pi)\}$ .

The left panel of Fig. 12 presents the difference between the TTV signals phases of the two planets – its deviation from 180 degrees; the value of  $\Delta_{a-ph} = 0$  means that the signals are in anti-phase – at the  $(e_1 \cos \phi_1, e_2 \cos \phi_2)$ -diagram. The white point denote the periodic configurations (for which  $\Delta_{a-ph} = 0$ ). The signals are in anti-phase not only for the periodic configuration, but also for the points lying at the line passing through the white point. Moreover, the other characteristics of the signals do not differ from the ones for the periodic configurations along this line. The right panel of Fig. 12 presents the amplitude of the outer planet's signal at the same diagram. Along the line defined by the condition of  $\Delta_{a-ph} = 0$ , the amplitude  $A_2$  is constant and equal to  $\approx 1.5$  minute.

There is another information in the right diagram, i.e., the ranges of the parameters for which the angles  $\Delta\omega$  and  $\phi_1$  oscillate. The  $\phi_2$  angle oscillates only in very tiny area around the white point (smaller than the size of the point at the plot). The analysis illustrated in Fig.12 shows that for certain systems which are far from periodic (including non-resonant ones), the TTV signals are identical as for the periodic configuration. In other words, the TTV signal is degenerated in a sense that it is possible to find very different orbital configurations which fit the observational data similarly well. Because of the size of the resonant region (in terms of the resonant angles librations) in the parameter space, one can expect that finding the periodic configuration as the best-fitting model of the TTV data is not very likely. More likely, the standard TTV analysis would find non-resonant systems with aligned apsidal lines  $\Delta\omega = 0$  as the true configuration.

In H5 there were performed tests which confirmed this presumption. Additionally, the weak dependence of the signals characteristics on the eccentricities (if only they lie at the line defined by  $\Delta_{a-ph} = 0$ ) may cause that the best-fitting models (e.g., in terms of the lowest  $\chi^2$  values) correspond to relatively high eccentricities ( $\sim 0.1$ ). In fact, the problem with finding real orbital structures of planetary systems has a wider context. Correct determination of the orbital parameters is a key issue for the studies of the formation of given configurations on the way of migration, because these parameters, taken as known from the observations, serve to find constraints on the migration parameters, and hence on the parameters of the protoplanetary discs. An incorrect determination of the parameters (and here the differences are qualitative from the point of view of the migration process) may result in wrong guidance of this kind of studies.

## Conclusions

The process of migration which leads to stable resonant systems (the periodic configurations in particular) made it possible to correctly interpret the astrometric data of the system of four massive planets around HR 8799 (article H1). It was shown that the system forms a chain of mean motion resonances 8:4:2:1, i.e., each subsequent pair of planets is involved in 2:1 MMR, as well as the whole system forms the four-body resonance. The system of this sort is stable and consistent with the observations.

In the scientific achievement, a strong relation between the migration of planets in protoplanetary discs and the structure of periodic configurations was demonstrated (articles H2, H3 and H4). It was shown that the families of periodic orbits determine the paths in the phase space along which the systems of migrating planets evolve. It was demonstrated that the smooth migration leads to formation of exact periodic configurations of the first order resonances, as well as the chains of such resonances. In the case of the second order resonance, approaching to the exact periodic configuration is in general more difficult. Nevertheless, it is possible that a given system is close-to-periodic.

Moreover, it was demonstrated in H5 that the Kepler-25 system may be a periodic configuration. Because of the TTV signal degeneration, the standard methods of the observational data analysis may lead to incorrect conclusions on the dynamical structure of particular systems. The analysis presented in H5 repeated for a greater number of systems could allow to find out how common are the periodic configurations among the known planetary systems and, as a consequence, to put constraints on the migration parameters.

The sample of the known systems of transiting planets includes at least a few systems whose TTVs could be modelled with the periodic configurations, as well as a number of systems for which it is not possible. The article (Panichi et al., 2019) presents an analysis of the KOI-1599 system with two planets close to 3:2 MMR, whose TTV signals differ in terms of the periodicity and the amplitudes with respect to what could be expected if the system was a periodic configuration. It was demonstrated that if the entrance into the resonance was sufficiently fast, a system formed in such a process would be shifted slightly with respect to the periodic configuration. It was shown that the observed TTV signals result from the semi-major axes modulations, not from the rotation of the system as a whole.

In contrast to the case of the Kepler-25 system, the period ratio of the KOI-1599 is very close to the nominal value of the resonance. As it was mentioned previously, in such a case the period of the rotation of the system as a whole (the super-period) is very long. If the system was not shifted with respect to the periodic configuration, the detection of any TTV variability would be impossible for the observing window of  $\sim 1500$  days, and thus the determination of the orbital and physical parameters of the system would not be possible either. The slight deviation of the system from the periodic configuration allows not only to estimate the migration parameters, but also helps to determine the parameters of the system itself.

The scientific achievement described in this document shows that understanding of the mechanical aspect of the migration (the role of the periodic orbits as attractors for the systems with migrating planets) allows to correctly determine the parameters of the observed systems. On the other hand, the systems characteristics obtained in this way (possibly a big number of them) could form the observational constraints for the astrophysical studies devoted to the discs structure as well as the planet-disc interactions.

A natural direction of the studies presented in scientific achievement is to analyse the TTV data of other systems with two and more planets discovered by the KEPLER mission and its successor, the K2 mission (Howell et al., 2014) as well as the TESS (Ricker et al., 2015) and PLATO (Rauer et al., 2014) missions. The aim of the future studies is to find how many systems could have been formed on the way of migration, as well as to put constraints on the parameters of this process.

#### 5. Discussion of other scientific and research (artistic) achievements:

Before receiving the doctoral degree I dealt with studies of the secular dynamics of non-resonant (hierarchical) planetary systems, which was the topic of my dissertation, as well as determination of the orbital and physical parameters of known planetary systems (mainly with a help of the analysis of the radial velocities of stars).

After obtaining the degree I focused on the evolution of planetary systems with energy dissipation, on the resonant dynamics as well as on the role of migration in the formation of mean motion resonances. Moreover, the analysis of the observed configurations was extended to different types of observations (mainly the transit timing). Below I present an overview of the articles published after receiving the doctoral degree, except the articles H1–H5 and the papers in which my contribution was small (below 10 per cent).

In (Migaszewski and Goździewski, 2011) the secular dynamics of a hierarchical system of three bodies within the post-Newtonian model of motion was studied. In particular, it was shown that the relativistic corrections are important in a wide range of the masses of the system. Moreover, the limitation of the applicability of the restricted model in cases of a low-mass outermost object was studied. A part of the results were described in the doctoral dissertation.

The article (Migaszewski, 2012) was the first paper of mine which goes beyond the conservative secular dynamics of planetary and stellar systems. In this work there are derived the equations of motion governing the evolution of the orbit as well as the rotation velocity vectors of two extended objects, whose figures are non-spherical due to their own rotations and well as the mutual tidal interactions. Moreover, the post-Newtonian corrections to the gravitation were accounted for. The model also assumes that the system dissipates the mechanical energy due to the tidal perturbation of the velocity field in the convective zones of the objects. The obtained equations of motion were used to study the dynamics of a system whose components have masses of the ones of the Sun and Jupiter, and the orbital period of the order of a few days.

In particular, the analysis was devoted to the boundary at the  $(a, e)$ -diagram for the planet fall onto the star, for different initial rotational periods of the star, inclinations of the orbit with respect to the stellar equator as well as for different values of the coefficients governing the efficiency of the energy dissipation in the objects. Moreover, the equilibrium corresponding to the synchronisation of the rotations of both the objects with the orbital motion was studied. It was shown that the equilibrium can be stable or unstable depending on the orbital size. In the latter case, a small deviation of the system from the equilibrium results in either falling the planet onto the star or an increase of the orbital size.

The article (Migaszewski et al., 2012) is devoted to the photo-dynamical analysis (i.e., fitting the dynamical model to the photometric data) of the six-planet system around Kepler-11 (Lissauer et al.,

2011). The masses of the planets as well as the orbital parameters were determined in this work. It was shown, in particular, that the relative inclinations between the orbits of planets b and c as well as planets d and e can be constrained dynamically with a good precision ( $<5^\circ$ ). Moreover, the structure of multi-body resonances was studied, as well as the dependence of the planets' densities on the orbital sizes was discussed.

The aim of the article (Migaszewski et al., 2013) was to test the hypothesis of linear spacing of the orbits of multi-planet systems (i.e., the sizes of subsequent orbits  $a_n \approx a_0 + n\Delta a$ ). Indeed, some of the known systems (e.g., Kepler-33) are characterised with this kind of the orbital structure. It was shown that for certain chains of mean motion resonances (e.g., 7:3, 5:3, 3:2, 4:3), the sizes of subsequent orbits can be approximated with a good precision by subsequent terms of an arithmetic progression. Although it seems that looking for statistical regularities of this sort in the known multi-planet configurations were premature, this article pointed my attention to the problem of migration and chains of mean motion resonances, which helped to develop the method described in H1.

In the next papers (Goździewski et al., 2016; Mills et al., 2016; Migaszewski et al., 2017; Panichi et al., 2018; Goździewski and Migaszewski, 2018), the problem of planetary migration is considered. The article (Goździewski et al., 2016) is devoted to the TTV analysis of the three-planet system around Kepler-60 (Steffen et al., 2012), a result of which was the masses and orbital parameters determination. The planetary migration was used here as a mechanism of elimination of a certain type of configurations consistent with the observations, i.e., the three-body resonance which is not a chain of two-body resonances. On the other hand, it was found that another configuration consistent with the TTV data (a chain of two-body resonances) is also consistent with the scenario of the migration-induced formation of the system.

The article (Mills et al., 2016) was mentioned already in this document when discussing the results of H1. The migration was used here as a process leading to the formation of chains of resonances, which resulted in finding a good starting point for further analysis of the light curve of the Kepler-223 system and determining the planets' masses as well as the orbital elements of this system.

The article (Migaszewski et al., 2017) is devoted to the TTV analysis of the two-planet system around Kepler-29 (Fabrycky et al., 2012) with the period ratio of  $\sim 9/7$ , in order to determine its physical and orbital parameters. It was shown that the analysis cannot give a unique set of the system's parameters. In particular, both close-to-circular orbits as well as the orbits of significant eccentricities  $\sim 0.3$ , are allowed by the observations. Moreover, the apsidal lines can be either aligned or anti-aligned ( $\Delta\omega \approx 0$  or  $\Delta\omega \approx \pi$ ). It was shown that the migration leads to the systems with  $\Delta\omega \sim \pi$  only, and with the eccentricities  $e \lesssim 0.02$ . It was also pointed out that some of the systems consistent with the observations are close to the periodic configurations. This work was a motivation for the studies of the migration-induced formation of 9:7 MMR (article H4).

The article (Panichi et al., 2018) is devoted to the TTV analysis of the three-planet system around Kepler-30 (Fabrycky et al., 2012). The parameters of the system were determined and it was shown that the system consists of the planets whose masses differ one from another significantly, from the planet of a mass of  $\sim 9 M_\oplus$  (the innermost one), through the planet of a mass of  $\sim 23 M_\oplus$  (the outermost one) to the very massive planet of a mass of  $\sim 1.7 M_{\text{Jup}}$  (the middle one). It was demonstrated that such a system could have been formed on the way of initially convergent migration, which became divergent. Moreover, the role of the three-body resonances during the divergent phase of the migration was pointed out.

The article (Goździewski and Migaszewski, 2018) was already mentioned when discussing the results of H1 in the context of refining the initial condition of the HR 8799 system by analysing the extended set of observations. Nevertheless, it was not the only goal of this work. Another aim was to study the

structure of the dust discs (belts) discovered in the inner as well as the outer parts of the system. The inner border of the outer disc was determined to be at  $\sim 145$  AU (Booth et al., 2016). However, this border is not consistent with the stability border in the system with the four known planets. In (Read et al., 2018) the influence of an additional exterior planet on the disc border was studied, concluding that a good agreement with the observationally determined border can be achieved for the additional planet of a mass of  $\sim 0.1 M_{\text{Jup}}$  in the orbit of  $a \sim 138$  AU. One of the results of (Goździewski and Migaszewski, 2018), was to show that the additional planet is not necessary for the reconstruction of the disc border. When assuming the migration of the four known planets from the orbits slightly wider than the ones presently observed, the inner border of the outer dust belt can be shifted up to the range determined in (Booth et al., 2016).

## References

- Baines E. K., White R. J., Huber D. et al. (2012), *ApJ*, 761:57.
- Batygin K. and Morbidelli A. (2013), *AJ*, 145:1.
- Beaugé C., Ferraz-Mello S. and Michtchenko T. A. (2003), *ApJ*, 593:1124–1133.
- Beaugé C., Michtchenko T. A. and Ferraz-Mello S. (2006), *MNRAS*, 365:1160–1170.
- Booth M., Jordán A., Casassus S. et al. (2016), *MNRAS*, 460:L10–L14.
- Borucki W. J., Koch D., Basri G. et al. (2010), *Science*, 327:977.
- Borucki W. J., Koch D. G., Basri G. et al. (2011), *ApJ*, 736:19.
- Chatterjee S. and Ford E. B. (2015), *ApJ*, 803:33.
- Contro B., Horner J., Wittenmyer R. A., Marshall J. P. and Hinse T. C. (2016), *MNRAS*, 463:191–204.
- Contro B., Wittenmyer Robert A., Horner J. and Marshall J. P. (2015), *Origins of Life and Evolution of the Biosphere*, 45:41–49.
- Cresswell P. and Nelson R. P. (2006), *A&A*, 450:833–853.
- D’Alessio P., Cantó J., Calvet N. and Lizano S. (1998), *ApJ*, 500:411–427.
- Delisle J. B. and Laskar J. (2014), *A&A*, 570:L7.
- Dittkrist K. M., Mordasini C., Klahr H., Alibert Y. and Henning T. (2014), *A&A*, 567:A121.
- Fabrycky D. C., Ford E. B., Steffen J. H. et al. (2012), *ApJ*, 750:114.
- Fabrycky D. C., Lissauer J. J., Ragozzine D. et al. (2014), *ApJ*, 790:146.
- Fabrycky D. C. and Murray-Clay R. A. (2010), *ApJ*, 710:1408–1421.
- Ferraz-Mello S., Beaugé C. and Michtchenko T. A. (2003), *Celestial Mechanics and Dynamical Astronomy*, 87:99–112.
- Goldreich P. and Tremaine S. (1979), *ApJ*, 233:857–871.
- Goldreich P. and Tremaine S. (1980), *ApJ*, 241:425–441.
- Götberg Y., Davies M. B., Mustill A. J., Johansen A. and Church R. P. (2016), *A&A*, 592:A147.
- Goździewski K., Breiter S. and Borczyk W. (2008), *MNRAS*, 383:989–999.
- Goździewski K. and Migaszewski C. (2009), *MNRAS*, 397:L16–L20.
- Goździewski K. and Migaszewski C. (2018), *The Astrophysical Journal Supplement Series*, 238:6.
- Goździewski K., Migaszewski C., Panichi F. and Szuszkiewicz E. (2016), *MNRAS*, 455:L104–L108.
- Hadjidemetriou J. D. (1976), *Astrophysics and Space Science*, 40:201–224.
- Hadjidemetriou J. D. and Voyatzis G. (2010), *Celestial Mechanics and Dynamical Astronomy*, 107:3–19.
- Howell S. B., Sobeck C., Haas M. et al. (2014), *Publications of the Astronomical Society of the Pacific*, 126:398.
- Kley W., Bitsch B. and Klahr H. (2009), *A&A*, 506:971–987.
- Lee M. H. and Peale S. J. (2002), *ApJ*, 567:596–609.
- Lissauer J. J., Fabrycky D. C., Ford E. B. et al. (2011), *Nature*, 470:53–58.
- Lithwick Y., Xie J. and Wu Y. (2012), *ApJ*, 761:122.

- Marois C., Macintosh B., Barman T. et al. (2008), *Science*, 322:1348.
- Marois C., Zuckerman B., Konopacky Q. M., Macintosh B. and Barman T. (2010), *Nature*, 468:1080–1083.
- Matsuyama I., Johnstone D. and Hartmann L. (2003), *ApJ*, 582:893–904.
- Michtchenko T. A. and Ferraz-Mello S. (2001), *Icarus*, 149:357–374.
- Migaszewski C. (2012), *Celestial Mechanics and Dynamical Astronomy*, 113:169–203.
- Migaszewski C. and Goździewski K. (2011), *MNRAS*, 411:565–583.
- Migaszewski C., Goździewski K. and Panichi F. (2017), *MNRAS*, 465:2366–2380.
- Migaszewski C., Goździewski K. and Słonina M. (2013), *MNRAS*, 436:L25–L29.
- Migaszewski C., Słonina M. and Goździewski K. (2012), *MNRAS*, 427:770–789.
- Mills S. M., Fabrycky D. C., Migaszewski C., Ford E. B., Petigura E. and Isaacson H. (2016), *Nature*, 533:509–512.
- Moore A., Hasan I. and Quillen A. C. (2013), *MNRAS*, 432:1196–1202.
- Nelson R. P. (2005), *A&A*, 443:1067–1085.
- Paardekooper S. J., Baruteau C., Crida A. and Kley W. (2010), *MNRAS*, 401:1950–1964.
- Paardekooper S. J., Baruteau C. and Kley W. (2011), *MNRAS*, 410:293–303.
- Panichi F., Goździewski K., Migaszewski C. and Szuszkiewicz E. (2018), *MNRAS*, 478:2480–2494.
- Panichi F., Goździewski K. and Turchetti G. (2017), *MNRAS*, 468:469–491.
- Panichi F., Migaszewski C. and Goździewski K. (2019), *arXiv e-prints*, arXiv:1901.01435.
- Papaloizou J. C. B. (2011), *Celestial Mechanics and Dynamical Astronomy*, 111:83–103.
- Papaloizou J. C. B. and Larwood J. D. (2000), *MNRAS*, 315:823–833.
- Pringle J. E. (1981), *Annual Review of Astronomy and Astrophysics*, 19:137–162.
- Rauer H., Catala C., Aerts C. et al. (2014), *Experimental Astronomy*, 38:249–330.
- Read M. J., Wyatt M. C., Marino S. and Kennedy G. M. (2018), *MNRAS*, 475:4953–4966.
- Ricker G. R., Winn J. N., Vanderspek R. et al. (2015), *Journal of Astronomical Telescopes, Instruments, and Systems*, 1:014003.
- Semenov D., Henning Th., Helling Ch., Ilgner M. and Sedlmayr E. (2003), *A&A*, 410:611–621.
- Shakura N. I. and Sunyaev R. A. (1973), *A&A*, 500:33–51.
- Sinclair A. T. (1975), *MNRAS*, 171:59–72.
- Snellgrove M. D., Papaloizou J. C. B. and Nelson R. P. (2001), *A&A*, 374:1092–1099.
- Steffen J. H., Fabrycky D. C., Ford E. B. et al. (2012), *MNRAS*, 421:2342–2354.
- Tanaka H., Takeuchi T. and Ward W. R. (2002), *ApJ*, 565:1257–1274.
- Tanaka H. and Ward W. R. (2004), *ApJ*, 602:388–395.
- Xu W. and Lai D. (2017), *MNRAS*, 468:3223–3238.
- Yoder C. F. (1979), *Nature*, 279:767–770.

Cezary Migaszewski